JOURNAL OF APPLIED ELECTROCHEMISTRY 25 (1995) 299–306

Characterization of a flow-by RVC electrode reactor for the removal of heavy metals from dilute solutions

E. J. PODLAHA,* J. M. FENTON

Department of Chemical Engineering, University of Connecticut, Storrs, CT 06269-3139, USA

Received 8 March 1994; revised 28 August 1994

Mass-transfer studies were carried out to characterize a porous, RVC, flow-by mode, single-pass reactor for the application of removing heavy metals from waste waters. Measurements of the limiting current and concentration for the reduction of the ferricyanide ion and copper ion respectively, show that the average mass-transfer coefficients were proportional to $Re^{0.7}$. The current was also monitored over extended periods of copper ion deposition to describe the plugging of the porous electrode.

1. Introduction

The removal of heavy metals from waste solutions is typically governed by mass transport limitations as the concentration of the metal ion becomes small. A three-dimensional reticulated vitreous carbon (RVC) electrode reactor can be used to effectively remove these metal ions from dilute solutions owing to its high surface area to volume ratio. The reactor investigated here consists of two RVC electrodes where the current and fluid flow are perpendicular, as opposed to a parallel configuration. This design, sketched in Fig. 1, has been shown to minimize potential drops in the reaction [1–5]. In this study the reactor is characterized by measuring average mass-transfer coefficients within a short time scale, and monitoring the cell current at longer time scales. The average mass-transfer coefficients, obtained under short metal deposition times to minimize changes in the electrode geometry, are determined from two independent reactions: the electrodeposition of copper ions and the reduction of ferricyanide ions. Geometric changes of the electrode occur when the deposition time of the copper ions is long so that electrode plugging can be observed.

Electrolytic processes using porous electrodes for heavy metal removal are economically competitive with other waste treatment designs. Bennion and Newman [6] found that for a fairly small porous, carbon electrode reactor the value of the recovered metal more than paid for the installation and operation of the cell. Wenger and Bennion [7] also showed that a flow-through porous electrode reactor was competitive with existing technology. A more recent analysis done by Ayres [8] compared the operating and capital costs of a porous, RVC electrolytic cell to the hydroxide precipitation method. The electrochemical metal removal and recovery was economically competitive with precipitation, and as the cost of sludge disposal in landfills increases, the electrodeposition method will become even more attractive.

A possible scheme for the electrolytic recovery of heavy metals is to reduce the metal ion at the cathode while simultaneously generating either oxygen or a concentrated metal stream at the anode. When the cathode becomes plugged with the deposited metal the flow of current is reversed so that the metal can be recovered in the form of a concentrated metal solution, impurity free, by using independent flow streams. It could be readily adapted to the electroplating industry where a single metal ion is present in the rinse system due to drag out from a plating bath.

The use of porous carbon electrodes for the removal of heavy metals has been discussed extensively in the literature. Flow-through arrangements, where the current flow is parallel to the fluid flow, have been investigated with various three-dimensional electrodes including granular graphite [6–9], polyurethane foam [10], and RVC [8, 11–13]. There have been several experimental investigations of the flow-by configuration, where the current and fluid flow are perpendicular. Experimental studies of flow-by porous electrodes include the use of particulate electrodes [14–16], copper screens [4], carbon felt [17, 18], foam materials [10, 19] and RVC [8, 20–22].

This study is an experimental investigation to characterize a flow-by, RVC electrode reactor, by measuring average mass-transfer coefficients using two different reactions, and observing the changing limiting current during copper ion deposition. This paper thus complements the average mass-transfer correlations described in the literature and addresses the importance of pore plugging in reactor design.

2. Experimental methods

The flow-by reactor design in this study was based on the criteria established by Fedkiw [1] and Risch and Newman [5]. Fedkiw [1], using average mass-transfer coefficients based on a collection of data from the

* Present Address: Laboratoire de Métallurgie Chimique, Ecole Polytechnique Fédérale de Lausanne, Département des matériaux, MX-C Ecublens, CH-1015 Lausanne, Switzerland.

0021-891X

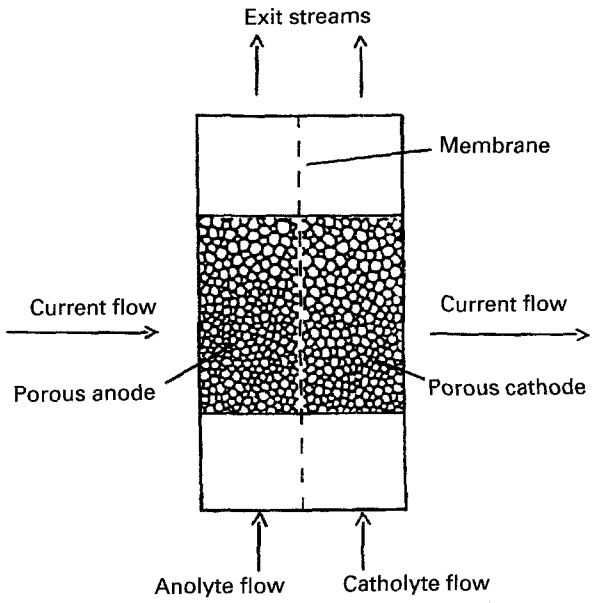

Fig. 1. Flow-by electrode configuration with the current and fluid flow perpendicular.

literature, has shown that given a maximum solution ohmic potential drop and reactant conversion, a flow-by reactor with an aspect ratio of the electrode length to thickness, $L/d > 5$, will produce a higher maximum processing rate than a flow-through configuration. Risch and Newman [5] established a design criteria that is independent of the choice of the average mass-transfer coefficient. At low conversion, a flow-by electrode is favourable as long as the L/d ratio is greater than one. At high conversions, a flow-by electrode configuration is favourable if the ratio $a_s K_m d/u < 2.218$, where u is the superficial velocity, a_s is the specific interfacial area and K_m is the average mass-transfer coefficient.

The cell contained two 45 grade, RVC (Electrosynthesis Co.) electrodes separated by a Nafion ion-exchange membrane (DuPont Co.). An interchangeable electrode design was developed to change the RVC electrode in case of plugging, or damage to the electrode matrix. This also allowed the length of the electrode to be varied.

Figure 2 shows a frontal view of the one half of the cell which includes the cell outer body made of PVC and the interchangeable electrode insert. The cell body was 45.7 cm long, 15.2 cm wide and 3.8 cm thick. A recess of 2.5 cm deep, 17.8 cm long and 8.9 cm wide was machined in the centre of the cell body in order to hold the interchangeable electrode insert. Each electrode insert was also constructed from PVC. A trough, with the dimensions of 1.5 cm deep and 4.5 cm wide was made lengthwise in the PVC of the electrode insert. The trough held a copper current collector plate and a graphite backing plate, each 0.32 cm thick, and the RVC electrode material. The dimensions and physical properties of the RVC electrode are given in Table 1. Spacers made from PVC were included to prevent solution from striking the ends of the carbon and copper plates. The length of the spacers depended upon the electrode length. For this study, two different electrode lengths were used, 5.1 and 10.2 cm.

The RVC material was glued with a graphite epoxy

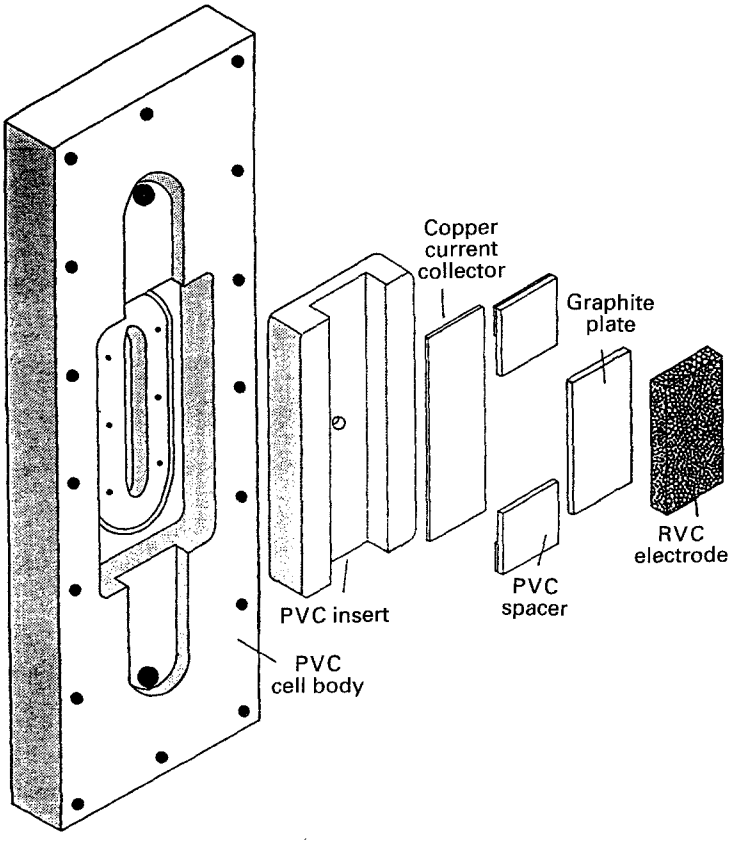

Fig. 2. Exploded view of cell half showing the electrode and electrode holder.

Table 1. RVC dimensions

Specific interfacial area, a_s/cm^{-1}	27.1
Porosity, ϵ	0.97
Electrode thickness, d/cm	0.87
Electrode width, w/cm	4.5

(Graphpoxy Grade PX, Dylon Industries, Inc.) to the graphite backing plate for support. The graphite epoxy was mixed with methyl ethyl ketone so that the epoxy could be easily spread onto the graphite plate. It was then necessary to bake the RVC-graphite plate for 4 h at 150 °C to cure the graphite epoxy. Once cooled the RVC-graphite plate was then attached with a silver epoxy (Traduct 2902, Tra-Con, Inc.) to the copper current collector. The copper plate was then glued to the bottom of the trough with a general purpose epoxy (Hardman epoxy 04007, Hardman, Inc.). A hole through the PVC insert and cell body allowed for an electrical connection to the copper current collector. The inserts were screwed into the outer cell bodies and two of the assembled cell body pieces, were bolted together, separated by the membrane. Details of the cell construction are given by Fenton, Grasso, and Podlaha [23].

The fluid flow circuit provided a continuous supply of reacting species to the electrode, as shown in Fig. 3. Ten litres of solution were held in a plastic tank above the cell. The flow stream from the tank was split into two streams so that fluid entering the anolyte and catholyte compartments of the cell was controlled independently. The flow rate was regulated by two flow meters (Gilmont Co.) in parallel for each electrode compartment. The flow outlets from the cell were returned to the holding tank where sufficient mixing took place by the action of bubbled nitrogen, although the primary use of the nitrogen was to displace dissolved oxygen. The flow rate at the working electrode was varied between 2.8 to 620 ml min^{-1} (0.012–2.6 cm s^{-1}). The flow rate at the counter electrode was maintained at the same flow rate as the working electrode.

Two different potentiostats (model 362 and model 371, EG&G Princeton Applied Research) were used depending on the current range measured. The model 362 was able to provide up to 1 A of current, and was used in the experiments to determine mass-transfer correlations. The model 371 provided up to 7 A, and was used for the experiments when deposition times were long and the copper ion concentration was high. The current was measured in real-time with an x–y–t recorder (model 200, Houston Instruments).

Copper ion solutions of variable concentrations of cupric sulfate, from 0.0001 M to 0.01 M, were used with a 0.8 M sodium sulfate supporting electrolyte at pH 3. The solution pH was adjusted with sulfuric acid. Ferricyanide reduction solutions consisted of 0.001 M potassium ferricyanide, 0.003 M potassium ferrocyanide and 0.5 M sodium hydroxide. All solutions were made with distilled, deionized water (Millipore Co.).

The properties of the electrolytic solution are given in Table 2. The solution conductivity and kinematic viscosity were measured using a YSI Scientific conductivity meter and a Canon–Fenske size 25 viscometer, respectively. The diffusion coefficients were determined with a platinum rotating disc electrode (RDE) system (Pine Instruments Co.). The RDE-analysis produced expected linear behaviour between the limiting current and the square root of the rotation rate. Since the values of all parameters did not change appreciably over the range of Cu^{2+} concentrations, average values were used. All experiments were carried out at room temperature.

The copper concentration was determined spectrophotometrically. A Bosch & Lomb Copper Spectrokit, Bincinchoninante reagent, was employed to detect Cu^{2+} species at a wavelength of 560 nm using a Milton Roy Spec 20 spectrophotometer. A linear relationship was found between the absorbance and concentration of Cu^{2+} below 10^{-4} M. All samples were diluted below this concentration for analysis. Accuracy was found to be within 2% when compared against copper reference standard solutions. It was

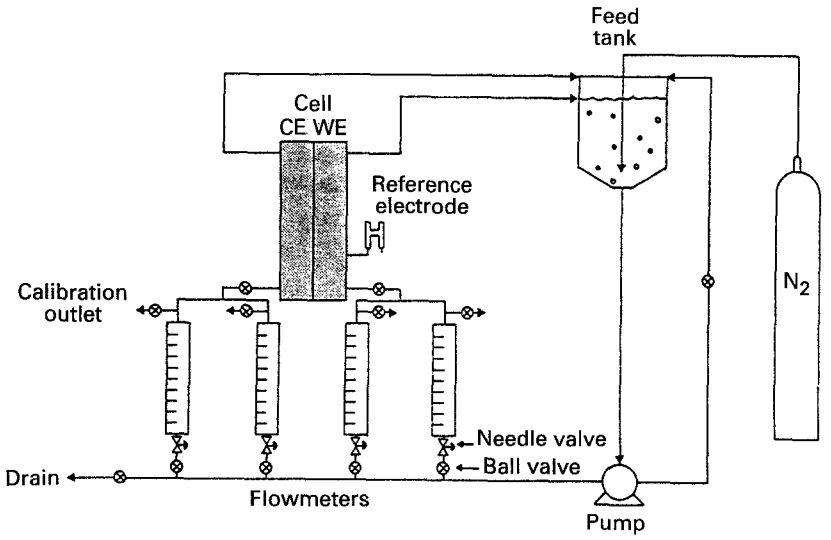

Fig. 3. Fluid flow schematic.

Table 2. Electrolytic solution properties

Property	*Copper deposition*	*Ferricyanide reduction*
Solution conductivity, $\kappa/\Omega^{-1}\,cm^{-1}$	0.078	–
Kinematic viscosity, $\nu/cm^2\,s^{-1}$	0.011	0.0105
Diffusivity, $D/cm^2\,s^{-1}$	4.5×10^{-6}	6.4×10^{-6}

observed that the concentration in the holding tank changed slightly during experimental operation. As a result, the inlet concentration to the reactor was measured for each run at each flow rate. Prior to electrolysis the RVC anode was plated with copper.

The following procedure was used to determine the average mass-transfer coefficient under short deposition times. A scan rate of $2\,mV\,s^{-1}$ was used to generate polarization curves, a plot of average current versus applied potential. The current scale is represented as current density by dividing the total current by the specific interfacial area and the electrode volume in all polarization curves presented here. The applied potential was then set to a value corresponding to the average limiting current, which was the region which possessed the minimum slope on the polarization plot. Copper ion concentration samples were then collected from the entrance and exit of the working electrode. The procedure was repeated for various flow rates and inlet copper ion concentrations with a constant electrode length of 10.2 cm.

Extended time deposition experiments were also carried out. The potential was fixed at −500 mV vs SCE. The bulk concentration and flow rate were kept constant at 0.034 M and $28.3\,ml\,min^{-1}$, respectively. The limiting current value was monitored over time to observe the electrode plugging-up with copper. Two different working electrode lengths were considered, 10.2 and 5.1 cm.

3. Results and discussion

3.1. *Short deposition times*

Figure 4 shows several average polarization curves for the copper sulfate system at a fixed feed Cu^{2+} concentration of 0.0023 M and various flow rates. At flow rates below $198.5\,ml\,min^{-1}$ ($0.85\,cm\,s^{-1}$), the average limiting currents are observed and increase with flow rate. The limiting current plateau becomes less distinct with increasing flow rate, and is slightly sloping indicating that the side reaction, hydrogen evolution, is contributing to the total cathodic current density. At large negative potentials, the side reaction becomes even more significant as the average cathodic current rises.

In Fig. 5, average polarization curves for the ferricyanide reduction are shown at a fixed concentration of 0.001 M. The average limiting currents are well defined even at high flow rates and increase as the flow rate increases. In this case the hydrogen side reaction is much lower due to the alkaline electrolyte.

Figure 6 is a plot of polarization curves for various inlet Cu^{2+} concentrations, at a constant flow rate of $65\,ml\,min^{-1}$ ($0.28\,cm\,s^{-1}$), where the y-axis has been normalized with respect to concentration. Depending on the relative rate of the main reaction, copper reduction, to the side reaction, hydrogen evolution, the average limiting currents for copper reduction may or may not be distinct. For example, at low inlet Cu^{2+} concentration of 1.2×10^{-4} M, the average limiting current for the cupric ion reduction is not distinct, and completely masked by the side reaction. At the higher inlet Cu^{2+} concentration of 2.3×10^{-3} M and 8.1×10^{-3} M the average limiting currents are more clearly defined and the inlet concentration normalized to concentration is roughly the same.

At the limiting current, I_{lim}, the reaction rate is controlled by mass-transfer. If the bulk concentration, C_b, does not change appreciably throughout the reactor and there is no side reaction then the average mass-transfer coefficient can be directly determined

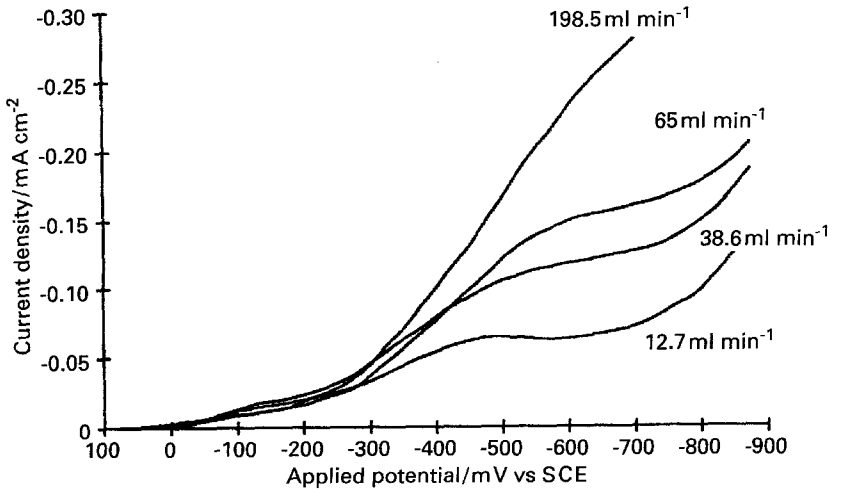

Fig. 4. Cupric sulfate reduction polarization curves for different flow rates at a constant Cu^{2+} concentration of 0.0023 M using the 10.2 cm length electrode.

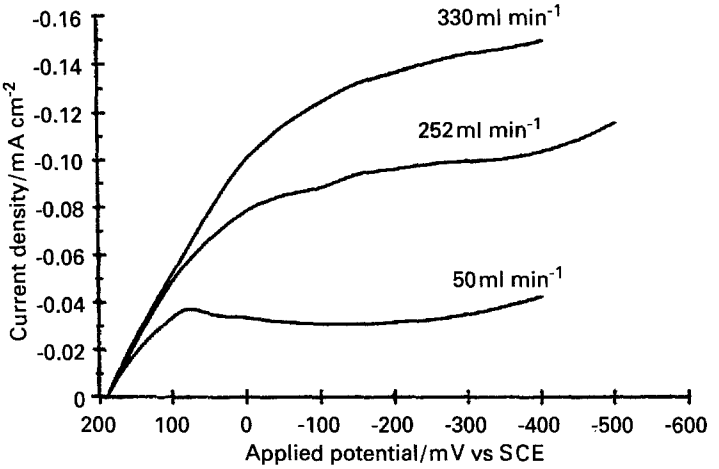

Fig. 5. Ferricyanide reduction polarization curves for different flow rates at a constant $Fe(CN)_6^{3-}$ concentration of 0.001 M and a 10.2 cm length electrode.

from the limiting current [10],

$$K_m = \frac{|I_{lim}|}{nFwdLa_sC_b} \quad (1)$$

where w is the electrode width.

However, in this study the bulk concentration can change dramatically throughout the reactor. Figure 7 depicts the cupric ion conversion, $1 - C_{b,out}/C_{b,in}$, with flow rate for different bulk, inlet concentrations, $C_{b,in}$, of Cu^{2+}. The data have been grouped into different ranges of inlet Cu^{2+} concentration. All experiments within a particular group were carried out with the same electrode and each electrode was constructed with the same dimensions and porosity grade RVC. The conversion of the cupric ion to solid copper ranges from over 90% down to below 20% with an exponential decrease of conversion with flow rate. Assuming axial diffusion and dispersion can be neglected so that plug flow prevails, and convection is the dominate mode of transport then the decrease in the cupric ion concentration at the reactor outlet is consistent with Equation 2 [6, 10, 24],

$$C(y) = C_{b,in}\exp\left(-\frac{a_sK_my}{u}\right) \quad (2)$$

When the average limiting current is indicative of only the main reaction, as in the case for the ferricyanide ion reduction, an average mass-transfer coefficient, taking into account the change in bulk concentration as the solution passes through the reactor, can be determined by integrating the cell current over the reactor, assuming concentration changes according to Equation 2.

$$K_m = -\frac{u}{a_sL}\ln\left(1 - \frac{|I_{lim}|}{nFwduC_{b,in}}\right) \quad (3)$$

It was evident that during copper deposition the reactor was not always operating at 100% current efficiency which is reflected in the poorly defined limiting currents shown in Figs 4 and 6. An alternative approach in determining the average mass-transfer coefficient is to use the concentration of Cu^{2+} at the inlet and outlet, $C_{b,out}$, of the reactor [24],

$$K_m = \frac{u}{a_sL}\ln\left(\frac{C_{b,in}}{C_{b,out}}\right) \quad (4)$$

The average mass-transfer coefficients were compared by relating the Sherwood number, $Sh = K_m\epsilon/a_sD$, to the Reynolds number, $Re = u/\nu a_s$ and the Schmidt number, $Sc = \nu/D$, in the form of a

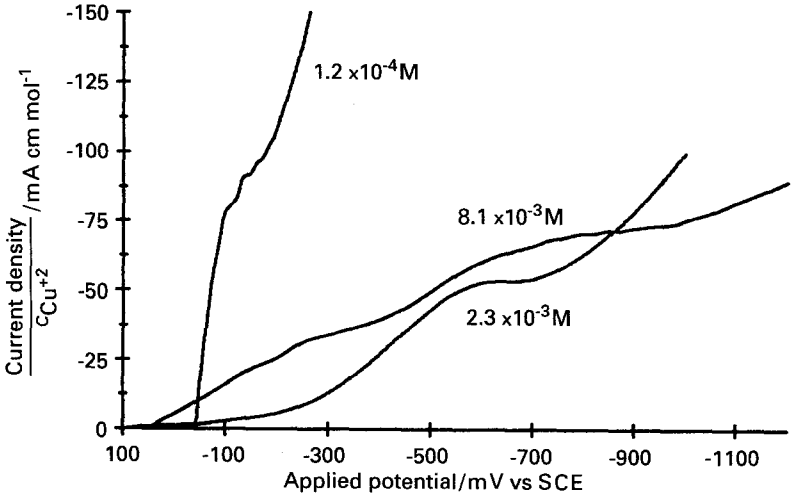

Fig. 6. Cupric sulfate reduction polarization curves for different inlet concentrations, at a flow rate of 65 ml min^{-1} (0.28 cm s^{-1}) and an electrode length of 10.2 cm.

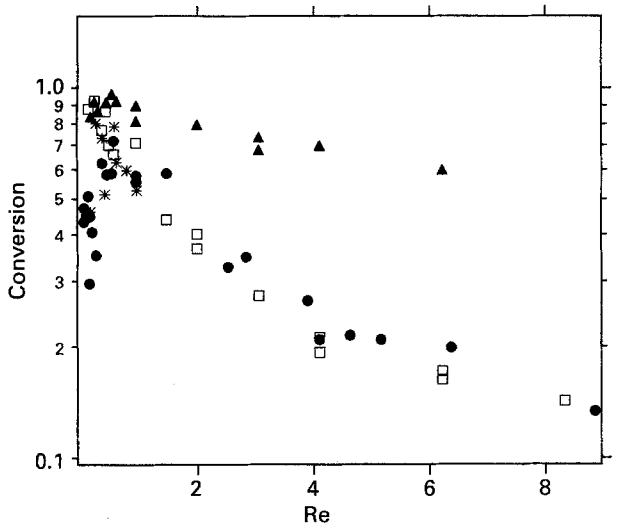

Fig. 7. Fractional conversion of cupric ion reduction to solid copper as a function of *Re* for different groups of data falling within a certain range of inlet concentration. Inlet Cu^{2+} concentration: (□) 0.0001, (●) 0.0015–0.0023, (▲) 0.003–0.004 and (*) 0.008–0.01 M.

power expression [24, 25],

$$Sh = bRe^{m}Sc^{1/3} \tag{5}$$

where D is the diffusivity and ν is the kinematic viscosity. A logarithmic plot of Sh against Re should produce a straight line with slope equal to m and intercept equal to log b, at a constant Sc.

Figures 8 and 9 are logarithmic plots of Sh against Re for the copper deposition reaction, utilizing Equation 4, and the ferricyanide reduction case, using Equation 3. A best fit line was used to correlate the data. The power relations are as follows:

$$\left.\begin{array}{ll} \text{for} \quad Cu^{2+} & Sh = 0.44\,Re^{0.69}Sc^{1/3} \\ \text{for} \quad Fe(CN)_6^{-3} & Sh = 0.23\,Re^{0.71}Sc^{1/3} \end{array}\right\} \tag{6}$$

The linear correlation coefficients are 0.821 and 0.952 for the copper and ferricyanide reduction, respectively. In order to try to explain the large scatter of

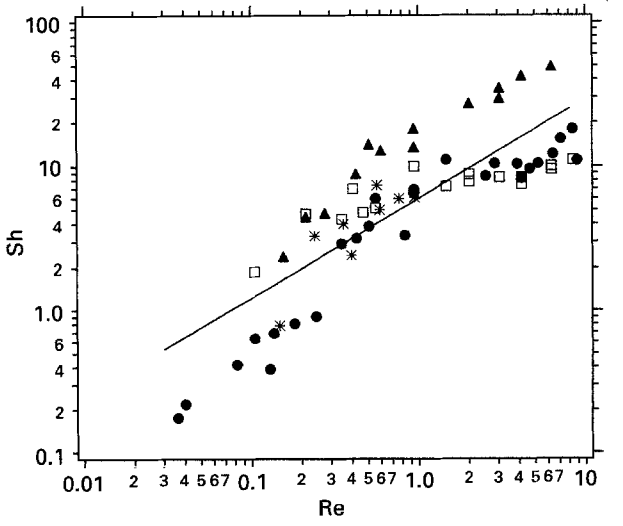

Fig. 8. Dimensionless mass-transfer (Sh) and flow rate (Re) correlation determined from copper reduction data. Inlet Cu^{2+} concentration; (□) 0.0001, (▲) 0.003–0.004, (●) 0.0015–0.0023 and (*) 0.008–0.01 M. (——) Best fit line.

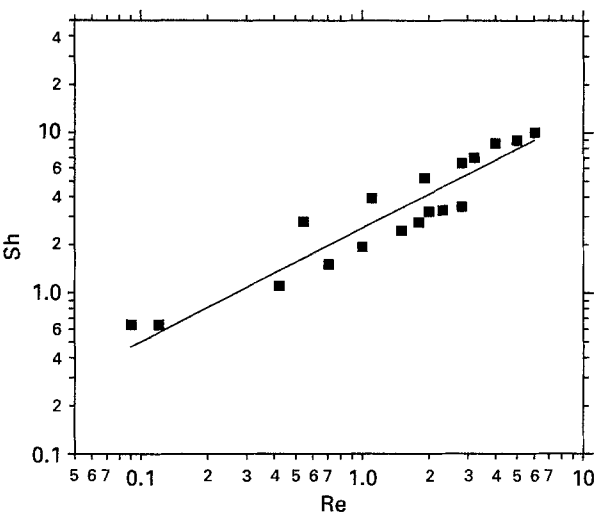

Fig. 9. Dimensionless mass-transfer (Sh) and flow rate (Re) correlation determined from ferricyanide reduction data.

data the experimental points have been grouped with respect to a range of inlet concentrations. Also all experiments within a group were performed with the same electrode. If a given group of experiments are considered then there is much less scatter of the data. One explanation for the discrepancies between the different groups could be due to differences in flow characteristics due to channeling or gas evolution. Additionally, the copper ion conversion, shown in Fig. 7, varies significantly. At low flow rates the conversion was high and mass-transport may be limited by the superficial velocity. Ideally, at 100% reactant conversion the maximum limiting current would be directly proportional to the solution flow rate, resulting in $m = 1$ [26]. At higher flow rate regimes $m < 1$. Therefore, the large differences in reactant conversion with flow rate can contribute to the low correlation in Equation 6 if the mass transport behaviour changes within the flow rate range investigated.

The dependence of the average mass-transfer coefficient with flow rate closely corresponds with the ferricyanide data. In this reactor we therefore find that $K_m \propto u^{0.7}$. These average mass-transfer correlations fall within the range of those reviewed by Fedkiw [1]. The power dependence of Re in this work is higher than in other correlations made with RVC and foam materials in flow-by reactors. In the work of Tentorio and Casolo–Ginelli [10] the exponent was found to be 0.49 and 0.53 for two different grades of RVC. Langlois and Coeuret [19] report values between 0.45 and 0.48 for different grades of nickel foam stacks. The exponent found in the study of Pletcher, Whyte, Walsh and Millington [20] was 0.48 determined from data taken with several different grades of RVC. In these studies, however, the reactant conversion was very low per pass compared to the reactant conversion in this investigation. The average mass-transfer dependence with flow rate here corresponds well with data obtained from flow-by, three-dimensional, carbon felt reactors, where the exponents, for example, have been found to be 0.61 or 0.72 [18] and between 0.61–0.76 [17]. In these studies

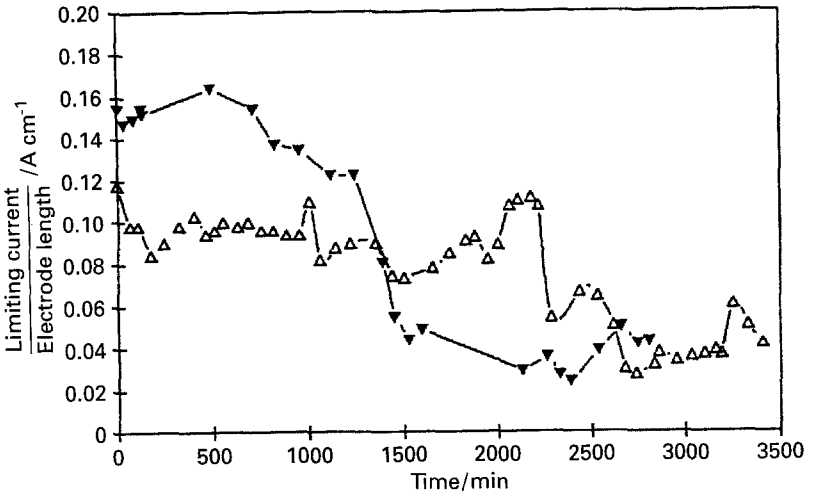

Fig. 10. Limiting current as a function of time during electrode plugging with an electrode length of 10.2 cm and 5.1 cm, cupric ion concentration of 0.034 M and a flow rate of 28.3 ml min^{-1} (0.12 cm s^{-1}). Electrode length: (▼) 10.2 and (△) 5.1 cm.

the superficial velocity was low and similarly the reactant conversion was high.

3.2. *Long deposition times*

In the previous Section polarization curves were generated under the assumption that the electrode area did not change appreciably. This assumption was valid since the time spent to complete a potential scan was very short, at most ten minutes. However, if the cell was operated for a longer time, pore plugging of the electrode becomes significant. Figure 10 is a plot of the average limiting current of the working electrode at −500 mV vs SCE over time with a constant flow rate of 28.3 ml min^{-1} (0.12 cm s^{-1}), a bulk concentration of 0.034 M and an electrode length of either 10.2 or 5.1 cm. The y-axis is scaled to the electrode length so that all the data can be plotted on a single graph. The greatest rate of copper removal for the 10.2 cm long electrode occurred between 0–1000 min. A sharp decrease in cathodic current is noted at approximately 1250 min. The average cathodic limiting current for the shorter electrode had a more gradual decrease. Both electrodes reach a constant limiting current after about 2500 min.

The highest reaction rate can be assumed to occur in the region near the entrance of the electrode, as implied by Equation 2. Most of the copper deposition will occur within a short distance of the electrode proportional to the superficial velocity divided by the specific interfacial area and the local mass-transfer coefficient. The additional electrode area helps to further decrease the copper ion concentration although the main reaction rate is lower and the current efficiency will be reduced due to the hydrogen evolution side reaction. In the shorter electrode, during a single-pass of electrolyte the total conversion of the copper ion reduction is lower compared to the longer electrode, since the residence time in the reactor is smaller. A more uniform distribution of copper should result in the direction parallel to electrolyte flow.

When the cell was disassembled copper was found deposited throughout the electrode length for both size electrodes [27]. A large excess of solid copper extended from the electrode entrance and exit of the longer, 10.2 cm, electrode. A more uniform reaction distribution for the shorter electrode was observed, without excess accumulation of copper at the electrode exit. Although pore plugging was significant at the electrode entrance, the copper deposition reaction continued at an approximately constant current achieved after 2500 min. An explanation for this steady limiting current is that during this time copper deposits predominantly at the entrance and exit cross-sectional regions of the electrode, caused by channeling of the fluid which is created by the partial plugging at the electrode entrance. There is now no benefit of having a porous electrode material and the entrance and exit planes of the electrode, as well as the channeling path, act as solid electrode surfaces.

Polarization curves were recorded at different times during the deposition experiment. Three of these curves are shown in Fig. 11 for the 10.2 cm length electrode. At the beginning of electrolysis the limiting current was not evident from the first polarization curve. At this low flow rate, 28.3 ml min^{-1} (0.12 cm s^{-1}), there is high reactant conversion so that near the electrode exit the relative rate of the hydrogen side reaction is large compared to the copper deposition reaction thus masking the copper deposition limiting current from the average polarization curve. As time progressed, the shape of the polarization curve changed. The second curve was taken after 13 h of electrolysis. This curve clearly shows a limiting current plateau. Due to the changes in electrode shape with time caused by plugging of the electrode pores a lower reactant conversion per pass is realized and an improvement of the ratio of the main reaction to the side reaction rate near the electrode exit results, producing the well defined average limiting current. The third curve was taken after 46 h of electrolysis and the value of the limiting current is significantly lowered, as a result of the decreased specific interfacial area.

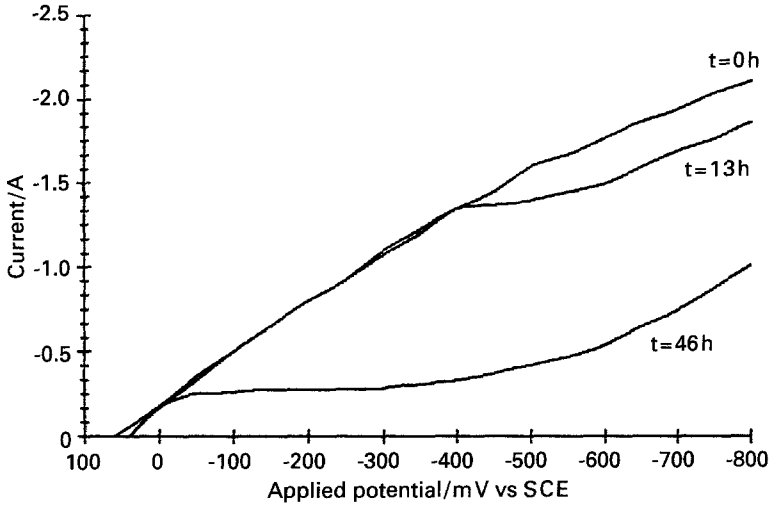

Fig. 11. Polarization curves taken at different times during the electrodeposition of copper which plugs the electrode pores, with a constant cupric ion concentration of 0.034 M, electrode length of 10.2 cm and flow rate of 28.3 ml min^{-1} (0.12 cm s^{-1}).

Excess gas formation can have the undesirable effect of breaking apart the porous matrix or blocking localized regions of the electrode surface, which can change the active specific interfacial area. However, these effects are considered small over long deposition times since there was no evidence of such phenomena when the cell was inspected upon disassembly.

The quality of solid, adherent copper that was plated in the reactor was granular and dull, typical of operating at the limiting current. This type of recovered material may be subsequently used as an anode in the reactor to create a concentrated copper stream, or the whole electrode can be discarded safely since the heavy metal is in a solid form.

4. Conclusions

A flow-by RVC electrode has been used effectively for the removal of copper ions from dilute solutions. Average mass-transfer correlations, to be used as a design aid, have been determined and show agreement with other literature findings. The relationship of the average mass-transfer coefficient with flow rate determined from the ferricyanide reaction and copper reduction are almost the same. This indicates that the assumption of negligible geometric changes during copper deposition for short times is valid. The reactor was also operated for a long time in order to plug up the electrode with copper. The measured current with time was found to drop sharply and reach a steady state, as the copper deposit filled the electrode pores.

Acknowledgements

This research was financed in part by the United States Department of Interior as authorized by the Water Research and Development Act of 1978 (P.L. 95-467).

References

[1] P. S. Fedkiw, *J. Electrochem. Soc.* **128** (1981) 831.
[2] J. A. Trainham and J. Newman, *Electrochim. Acta* **26** (1981) 455.
[3] R. Alkire and P. K. Ng, *J. Electrochem. Soc.* **121** (1974) 95.
[4] *Idem, ibid.* **124** (1977) 1220.
[5] T. Risch and J. Newman, *ibid.* **131** (1984) 2551.
[6] D. N. Bennion and J. Newman, *J. Appl. Electrochem.* **2** (1972) 113.
[7] R. S. Wenger and D. N. Bennion, *ibid.* **6** (1976) 385.
[8] J. L. Ayres, PhD dissertation, University of North Carolina (1986).
[9] K. P. Chu, M. Fleischmann and G. J. Hills, *J. Appl. Electrochem.* **4** (1974) 69.
[10] A. Tentorio and U. Casolo-Ginelli, *ibid.* **8** (1978) 195.
[11] M. Fleischman and A. Saraby-Reintjes, *Electrochim. Acta* **29** (1984) 69.
[12] M. Matlosz and J. Newman, *J. Electrochem. Soc.* **133** (1986) 1851.
[13] J. Wang and H. D. Dewald, *J. Electrochem. Soc.* **130** (1983) 1814.
[14] A. Storck, M. A. Enriquez-Granados, M. Roger and F. Coeuret, *Electrochim. Acta* **27** (1982) 293.
[15] B. J. Sabacky and J. W. Evans, *J. Electrochem. Soc.* **126** (1979) 1176.
[16] G. Kreysa, Habilitation Schrift, Dortmund University (1977).
[17] A. M. Polcaro and S. Palmas, *in* 'Electrochemical Engineering and the Environment 92', Institute of Chemical Engineers of Great Britain (1992), p. 85.
[18] K. Kinoshita and S. C. Leach, *J. Electrochem. Soc.* **129** (1982) 1993.
[19] S. Langlois and F. Coeuret, *J. Appl. Electrochem.* **19** (1989) 51.
[20] D. Pletcher, I. Whyte, F. C. Walsh and J. P. Millington, *ibid* **21** (1991) 659.
[21] D. Pletcher, I. Whyte, F. C. Walsh and J. P. Millington, *ibid* **21** (1991) 667.
[22] D. Pletcher, I. Whyte, F. C. Walsh and J. P. Millington, *ibid.* **23** (1993) 82.
[23] J. M. Fenton, D. T. Grasso and E. J. Podlaha, *J. Electrochem. Soc.* **137** (1990) 2809.
[24] J. S. Newman and W. Tiedemann in 'Advances in Electrochemistry and Electrochemical Engineering', vol. 11 (edited by H. Gerischer and C. W. Tobias), John Wiley & Sons, New York, (1978), p. 364.
[25] R. B. Bird, W. E. Stewart and E. N. Lightfoot, 'Transport Phenomena', John Wiley & Sons, New York (1960), p. 645.
[26] R. Alkire and B. Gracon, *J. Electrochem. Soc.* **122** (1975) 1594.
[27] E. J. Podlaha, MS thesis, University of Connecticut (1989), p. 91 and p. 93.